LightSAR Pushes both the Technology and the Economics

Steven Bard, Ph.D.

California Institute of Technology

Jet Propulsion Laboratory

As part of the strategic plan for its Earth Science Enterprise, the U.S. National Aeronautics and Space Administration (NASA) is committed to fostering the development and prosperous use of imaging radar science and technology in both the public and private sectors. Past spaceborne and airborne short-duration radar missions have firmly established the vast potential of imaging radar for expanding scientific knowledge of the Earth, as well as other planets. Now NASA is proposing an affordable, continuously Earth-orbiting imaging radar that will deliver exciting Earth science data with even greater usefulness in commercial applications.

The proposed imaging radar spacecraft is called LightSAR, for Lightweight Synthetic Aperture Radar. LightSAR will orbit Earth for five years, making continuous observations of the surface. It will use advanced technologies to reduce the cost and enhance the quality of radar-based information. Because it will be capable of imaging with multiple frequencies, multiple polarizations, and variable imaging swaths, and because its orbit will allow it to image almost every location on Earth each day, LightSAR's capabilities will be adaptable to a wide range of applications, many of which have no doubt yet to be discovered.

A mission such as LightSAR offers important benefits to both the science community and U.S. industry. Thus, an innovative government-industry teaming approach is being explored, with industry sharing the cost of development in return for commercial rights to mission data. The Jet Propulsion Laboratory (JPL) in Pasadena, California, is leading the development of LightSAR for NASA, in collaboration with NASA's Stennis Space Center (in southern Mississippi) and four industry teams. They hope to find ways to jointly fulfill both strategic science goals and commercial remote sensing needs. Their focus has been to design, develop, and launch by 2002 a high-performance SAR spacecraft for about one-fourth the cost of previous free-flying SAR missions. These cost reductions will be achieved by combining the use of advanced technologies; a commercial spacecraft; established launch vehicle and operations practices, services, and infrastructures; "faster, better, cheaper" management; and an innovative government-industry partnership.

A Technological Jump

Technology developments incorporated into the SAR payload design include advanced microelectronics and lightweight materials that enable significant performance enhancements over previous SAR instruments, at a total payload mass of under 250 kg. This low mass enables the LightSAR spacecraft to be launched on a small launch vehicle such as a Taurus XL or LMLV-2.

The information from LightSAR could potentially be used to address a whole range of practical issues, including:

- Measuring ground surface displacement, to provide insight into earthquakes and volcanoes and support emergency management efforts.
- Producing maps of vegetation and land cover to assess land use patterns and change for agricultural, wildlife, and forest management applications.
- Studying the movements and changing size of glaciers and ice floes to help better understand long-term climate variability.
- Developing highly detailed and accurate elevation maps and charts for a wide range of military and civilian uses.
- Monitoring floods or assessing where they are most likely to occur.
- Assessing terrain for oil or mineral resource possibilities, or to inventory and characterize abandoned mine lands.
- Recognizing oil spills early and monitoring them to aid in containment efforts.
- Assessing the health of crops and forests.
- Planning urban development and understanding its likely effects.
- Imaging areas of archaeological interest in support of research on ancient civilizations.

LightSAR combines specific technologies that will enable it support a wide variety of applications.

Mapping Seismic Displacement with Unprecedented Accuracy

Over the past two decades, space geodetic techniques, in particular, the Global Positioning Satellite (GPS) system, have proven powerful in studying movements and deformations of the Earth's surface, leading to major advances in our ability to quantitatively model these effects. But these measurements lack spatial continuity and require field equipment at each study site.

Recent technological advances in spaceborne radar interferometry have permitted observation of mm-level surface deformation at 25-m resolution all over the globe. This technology was used to derive the first differential interferometric maps of the co-seismic displacement of the surface during the June 28, 1992, quake at Landers, California.

Nevertheless, at present, civilian spaceborne differential interferometry remains primarily a demonstration tool, because no mission dedicated to that purpose exists. Thus, one of the high-priority scientific goals of LightSAR is to refine our understanding of the earthquake cycle through mm-level interseismic and co-seismic vector deformation maps along faults and plate boundaries. With this use in mind, LightSAR is planned to include an L-band sensor and use a repeat-pass interferometry technique with multiple polarization modes.

In addition, LightSAR will allow the repeated measurement of surface change in seismically active areas along all continental margins and will be able to target new and previously unidentified areas of study. It will be able to image any particular area every 8 days, or all areas every 24 days.

Monitoring Rapidly-occurring Volcanic Events

Another high-priority scientific goal of LightSAR is to gather data for mm-level deformation maps to monitor volcanoes for new activity and the potential for imminent eruption.

The major observations in volcanology to be obtained by LightSAR are:

- The spatial and temporal extent of deformation of the surface before and during eruptions. These are the key measurements used as input to models of magma migration.
- The spatial extent of new material produced during an eruption, derived from image decorrelation, an important diagnostic of the eruption process.

Surface change caused either by the emplacement of new lava flows or by the collapse of volcanic craters, can be studied via the decorrelation of radar phase information at a spatial resolution of ~25 m/pixel. Specific high-priority volcanoes (for example, those in eruption or experiencing a "volcanic crisis" prior to eruption) may be imaged every orbit, while other areas can be imaged as few as four times per year.

To support these volcanological studies, in addition to the use of L-band radar and repeat-pass interferometric techniques, LightSAR will have an operational mode that will allow a 110-km-wide strip of data (using HH polarization) to be acquired continuously at a resolution of at least 25 meters and a phase accuracy that will still allow a surface displacement resolution of 2-5 mm statistical height over any swath.

Measuring Biomass for Carbon Cycle-related Prediction

Another important use of LightSAR data is in monitoring the global carbon cycle. The carbon cycle, especially as it affects concentrations of carbon dioxide and its role as a greenhouse gas, is fundamental to the study of Earth's climate. Carbon is stored in the form of plant material. Biomass is the weight of plant material, minus the water it contains, per a given area of land.

The seasonal growth of terrestrial plants, and forests in particular, leads to the temporary storage of large amounts of carbon, which could directly affect changes in global climate. In order to accurately predict future global change, scientists need detailed information about current distribution of vegetation types and the amount of biomass present around the globe. Optical techniques to determine net biomass don't work very well if the area being imaged is often covered by clouds. Imaging radar, however, can penetrate through cloud-cover with hardly any loss of information.

Among remote sensing instruments, radar has been shown to have the unique abilities to respond to biomass over a usable range and give reliable temporal information, because it sees through cloud cover. For an L-band radar, biomass values of up to 150-200 tons/hectare have been successfully retrieved.

Change in land cover is one of the fundamental factors perturbing the global carbon cycle. In addition to identifying primary land conversion, successful efforts are under way using SAR to estimate regrowth in secondary forests, a key factor in carbon balances. LightSAR's use of the longer L-band wavelength will enable monitoring of patterns of forest regrowth after disturbances such as fires or clear cutting. LightSAR is designed to meet the requirements for image

resolution so that the boundaries between growth and no-growth areas can be accurately distinguished and mass per unit area can be accurately assessed.

Wide-swath Continuous Monitoring for Oil Spills

Many forms of oil, from both biological and petroleum sources, smooth out the ocean surface, causing the area to appear dark in radar images. Thus, radar images are useful for detecting and measuring the extent of oil seepages on the ocean surface, from both natural and industrial sources.

With its continuous imaging of every potential location of oil spillage, LightSAR will give environmentalists and oil platform and shipping operators the data they need to monitor spills and mount containment efforts. It will provide long-term, high-resolution data on dispersal of oil slicks, as well as information about natural sources of oil slicks.

LightSAR's wide-swath, dual polarization (HH/VV) mode will support such studies of ocean features. This mode will allow a 250-500-km swath to be imaged continuously with a spatial resolution of at least 100 m.

Data of Many Uses

These and several of the other potential applications of LightSAR data are described on the LightSAR home page, at http://lightsar.jpl.nasa.gov.

Technical Summary of LightSAR Mission Design

LightSAR will generate data for commercial, Earth science, and civilian applications.

LightSAR will enable unique capabilities, including—

- Mapping of surface change. LightSAR's repeat-pass interferometry technique will enable continuous monitoring of Earth's dynamic topography to a height accuracy of within a few millimeters.

- Better discrimination of texture and water content. Longer (L-band) wavelength radar and use of multiple polarization modes will allow better distinction of textures, vegetation structures and water content, soil moisture, ice thickness, and numerous other applications.

- Long-term observations. Mission life expectancy is five years.

- Higher-resolution images. Imaging swaths of 100-km (60 miles) wide will provide 25-m (about 83-foot) horizontal resolution, accurate to within a few millimeters vertically. Even higher resolution, 1-3 meters (3-10 feet), is being considered in order to provide opportunities for additional commercial applications, such as detailed topographic mapping.

- Continuous monitoring of changing conditions. LightSAR's 8-10-day repeating, near-polar orbit (determined by the Global Positioning System, GPS), will provide visibility of most locations on Earth about once each day.

Characteristics of LightSAR design concepts under study include . . .

- State-of-the-art technologies with significant reduction in mass, as well as instrument and mission life-cycle costs.

- L-band, multipolarization, high-performance SAR with multiple resolutions and swath imaging capabilities. X-band or C-band is being considered for very high-resolution commercial applications.

Multiple Imaging modes:

- Spotlight
- High-resolution Strip
- Dual Polarization
- Quad Polarization
- Repeat Pass Interferometric
- ScanSAR

Aspect: Right or left looking.

Frequency: 1.2575 GHz (L-band), 9.6 GHz for potential addition of X-band or 5.3 GHz for C-band.

Antenna: Electronic beam steering to maximize the targetable swath.

Electronics may include a cross-link transceiver/timing synchronizer to accommodate future synchronization of two radar platforms for real-time interferometry.

Five commandable bandwidths to optimize resolution and data rate vs. incidence angle.

Antenna size: 10.8 m (azimuth) x 2.9 m (elevation) for L-band. Not yet determined for X- or C-band.

Polarization: HH, HV, VH, VV for L-band. Not yet determined for X- or C-band.

Peak power: 8,000 W.

Pulse width: 15, 3 μsec.

Nominal PRF: 1,600 Hz.

Sample size (bits/sample): 8,4 (BFPQ), 4 (no BFPQ).

Launch 2001/2002 time frame.

References

1. Abdelsalam, M, and R. Stern, "Mapping Precambrian structures in the Sahara Desert with SIR-C/X-SAR Radar: The Neoproterozoic Keraf Suture, NE Sudan," *J. Geophys. Res.*, vol. 101, no. E10, pp. 23063-23076, 1996.
2. Anys, H., and D. He, "Evaluation of textural and multipolarization Radar features for crop classification," *IEEE Trans. Geosci. Remote Sensing*, vol. 33, no. 5, pp. 1170-1181, 1995.
3. Beaudoin, A., et al., "Retrieval of forest biomass from SAR data," *Int. J. Remote Sensing*, vol. 15, pp. 2777-2796, 1994.
4. Dubois, P., J. van Zyl, and T. Engman, "Measuring soil moisture with imaging Radars," *IEEE Trans. Geosci. Remote Sensing*, vol. 33, no. 4, pp. 915-926, 1995.
5. Evans, D., et al., *Spaceborne Synthetic Aperture Radar: Current Status and Future Directions*, NASA Technical Memorandum 4679, 171 pgs., 1995.
6. Forget, P., and Pierre Broche, "Slicks, waves, and fronts observed in a sea coastal area by an X-band airborne synthetic aperture Radar," *Remote Sensing Environ.*, vol. 57, no.1, pp. 1-12, 1996.
7. Gabriel, A. G., R. M. Goldstein, and H. A. Zebker, "Mapping small elevation changes over large areas: Differential radar interferometry," *J. Geophys. Res.*, vol. 94, pp. 9183-9191, 1989.
8. Interagency Ad Hoc Working Group on SAR, *Operational Use of Civil Space-based Synthetic Aperture Radar (SAR)*, JPL Publication 96-16, 1996.
9. Izenberg, N.R., R.E. Arvidson, R.A. Brackett, S.S. Saatchi, G.R. Osburn, and J. Dohrenwend, "Erosional and depositional patterns associated with the 1993 Missouri River floods inferred from SIR-C and TOPSAR radar data", *J. Geophys. Res.*, vol. 101, pp. 23,149-23,168, 1996.
10. Kasischke, E., N. Christensen, and L. Borgeau-Chavez, " Correlating Radar backscatter with components of biomass in loblolly pine forests," *IEEE Trans. Geosci. Remote Sensing*, vol. 33, no. 3, pp. 643-659, 1995.
11. Massonnet, D., P. Briole, and A. Arnaud, "Deflation of Mount Etna monitored by spaceborne radar interferometry," *Nature*, vol. 375, pp. 567-570, 1995.

12. Moghaddam, M., and S. Saatchi, "Analysis of scattering mechanisms in SAR imagery over boreal forest: Results from BOREAS'93," *IEEE Trans. Geosci. Remote Sensing*, vol. 33, no. 5, pp. 1290-1296, 1995.

13. Peltzer, G., P. A. Rosen, "Surface displacement of the 17 May 1993 Eureka Valley, California, earthquake observed by SAR interferometry," *Science*, vol. 268, p. 1333, 1995.

14. Rosen, P., S. Hensley, H. Zebker, and F. Webb, "Surface deformation and coherence measurements of Kilauea volcano, Hawaii, from SIR-C Radar interferometry," *J. Geophys. Res.*, vol. 101, no. E10, pp. 23109-23125, 1996.

15. Shi, J., and J. Dozier, "Inferring snow wetness using C-band data from SIR-C's polarimetric synthetic aperture Radar," *IEEE Trans. Geosci. Remote Sensing*, vol. 33, no. 4, pp. 905-914, 1995.

16. Zebker, H. A., P. A. Rosen, R. M. Goldstein, A. Gabriel, C. L. Werner, "On the derivation of co-seismic displacement fields using differential radar interferometry: The Landers earthquake," *J. Geophys. Res.*, vol. 99, p. 19617, 1994.

17. Zebker, H. A., P. A. Rosen, S. Hensley, P. J. Mouganis-Mark, "Analysis of active lava flows on Kilauea Volcano, Hawaii, using SIR-C radar correlation measurements," *Geology*, vol. 24, p. 495, 1995.

Dr. Steven Bard is the LightSAR Project Manager at NASA's Jet Propulsion Laboratory in Pasadena, California, USA.

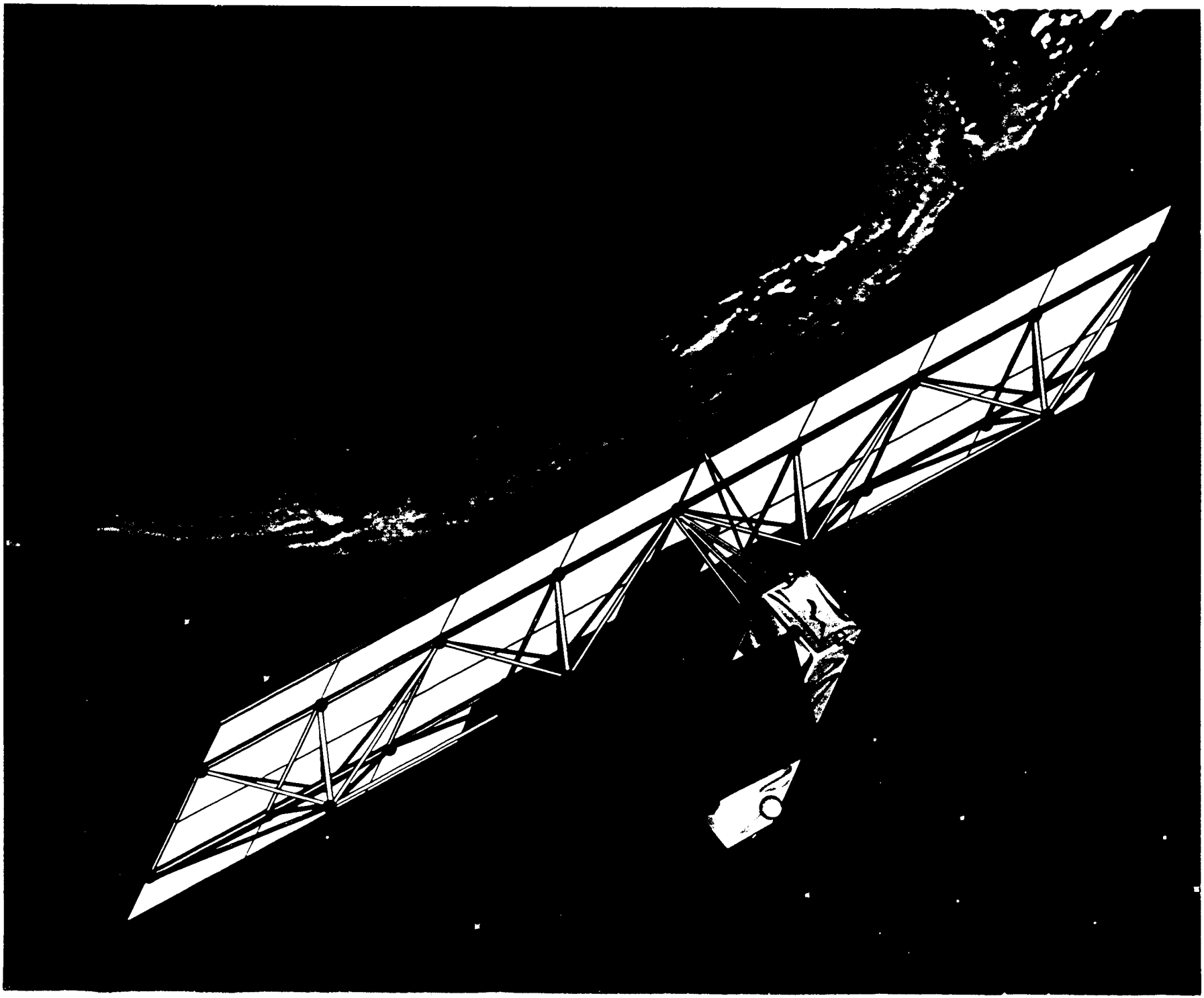

P-47286

Artist's rendering of proposed LightSAR spacecraft in Earth orbit.

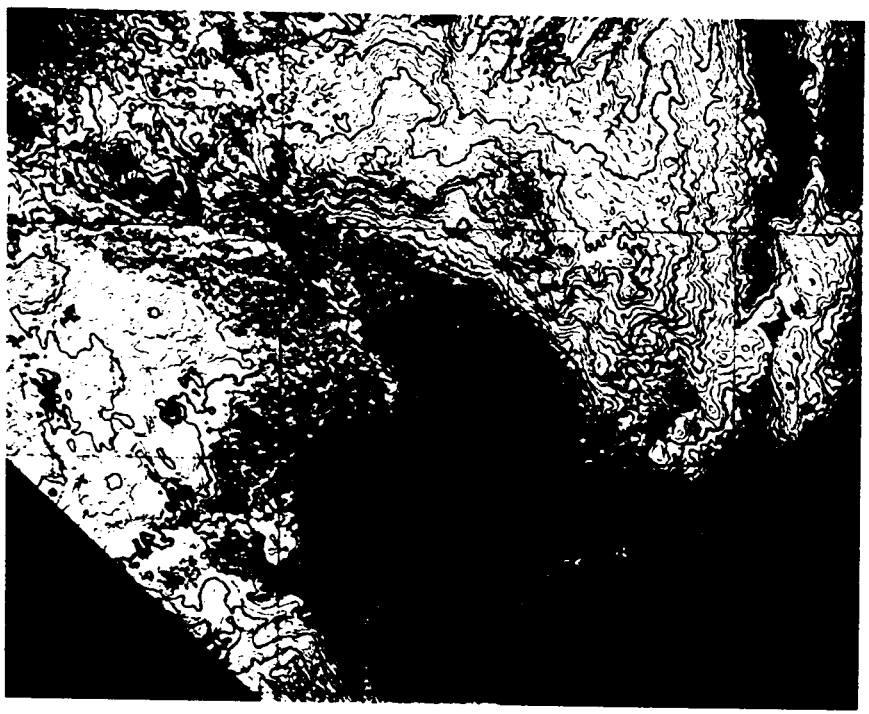

P-44941

These four SIR-C/X-SAR images of the Long Valley region of east-central California illustrate the steps required to produce three-dimensional data and topographic maps from radar images using interferometry. The image in the upper left shows L-band radar image data. The image in the upper right is an interferogram of the same area, made by combining L-band data from the two SIR-C/X SAR flights (April and October 1994). The colors in this image represent the difference in the phase of the radar echoes obtained on the two flights.

The image in the lower left shows a topographic map derived from the interferometric data. The image in the lower right is a three-dimensional perspective view of the northeast rim of the Long Valley caldera, looking toward the northwest. To create this image, SIR-C C-band radar image data are draped over topographic data derived from the interferometry processing.

SURFACE DISPLACEMENTS OF THE 1994 NORTHRIDGE M6.7 EARTHQUAKE

JERS-1 TWO-PASS RADAR INTERFEROMETRY

JPL

Rosen et al. 1995

P-45723

This image shows surface displacements resulting from the 1994 6.7 magnitude Northridge, California, earthquake. The area was imaged before and after the earthquake by the JERS-1 SAR system. The before and after images were combined with USGS digital elevation models to create the interferogram shown here. In the interferogram, color indicates the amount of surface displacement attributable to the earthquake. This displacement ranges from 0 centimeters (shown in the light purple) to 60 centimeters or just under two feet (shown in the deep red).

Kliuchevskoi Volcano, Kamchatka, Russia

September 30, 1994

Shuttle Photograph

SIR-C/X-SAR Radar Image

P-45734

This comparison shows photographic and radar images of the Kliuchevskoi volcano in Kamchatka, Russia, which began to erupt on September 30, 1994, as the second SIR-C/X-SAR space shuttle mission was beginning.

In the optical image on the left, the ash plume, which rose to an altitude of more than 18 kilometers (50,000 feet), is emerging from a vent on the north flank of Kliuchevskoi. In fact, the plume and its shadow partially hide the volcano itself.

In the radar image at right, Kliuchevskoi is the blue triangular peak in the center of the image, towards the left edge of the bright red area, which is bare snow cover. This eruption of Kliuchevskoi ejected massive amounts of gas, vapor, and ash. Melting snow mixed with volcanic ash triggered mudflows on the flanks of the volcano, which you can see as thin lines in various shades of blue and green on the north flank in the center of the image.

In addition to Kliuchevskoi, two other active volcanoes are visible in the image.

SIR-C/X-SAR

PRINCE ALBERT, SASKATCHEWAN, CANADA

APRIL 10, 1994

SIR-C IMAGE

LHH

LHV

CVV

BIOMASS MAP

0-50 tons/Ha

50-100 tons/Ha

100-150 tons/Ha

> 150 tons/Ha

P-43942

The image on the right is a biomass map of Prince Albert boreal forest in the Saskatchewan province of Canada. The map was produced from data acquired by the Spaceborne Imaging Radar aboard the shuttle Endeavor on its 20th orbit. Scientists from NASA, Goddard Space Flight Center and Jet Propulsion Laboratory used the SIR-C L-band and C-band data (image on left) to generate this biomass map. The area imaged is near the southern limit of the boreal forest and is part of a larger study area used in BOREAS (Boreal Ecosystem Atmospheric Study) project which was initiated by NASA and an international science team in the summer of 1993.

P-46293

SIR-C/X-SAR radar image of an offshore drilling field about 150 km (93 miles) west of Bombay, India, in the Arabian Sea. The dark streaks are extensive oil slicks surrounding many of the drilling platforms, which appear as bright white spots. The larger dark patches are dispersed slicks that were likely discharged earlier than the longer streaks, when the winds were probably from a different direction.